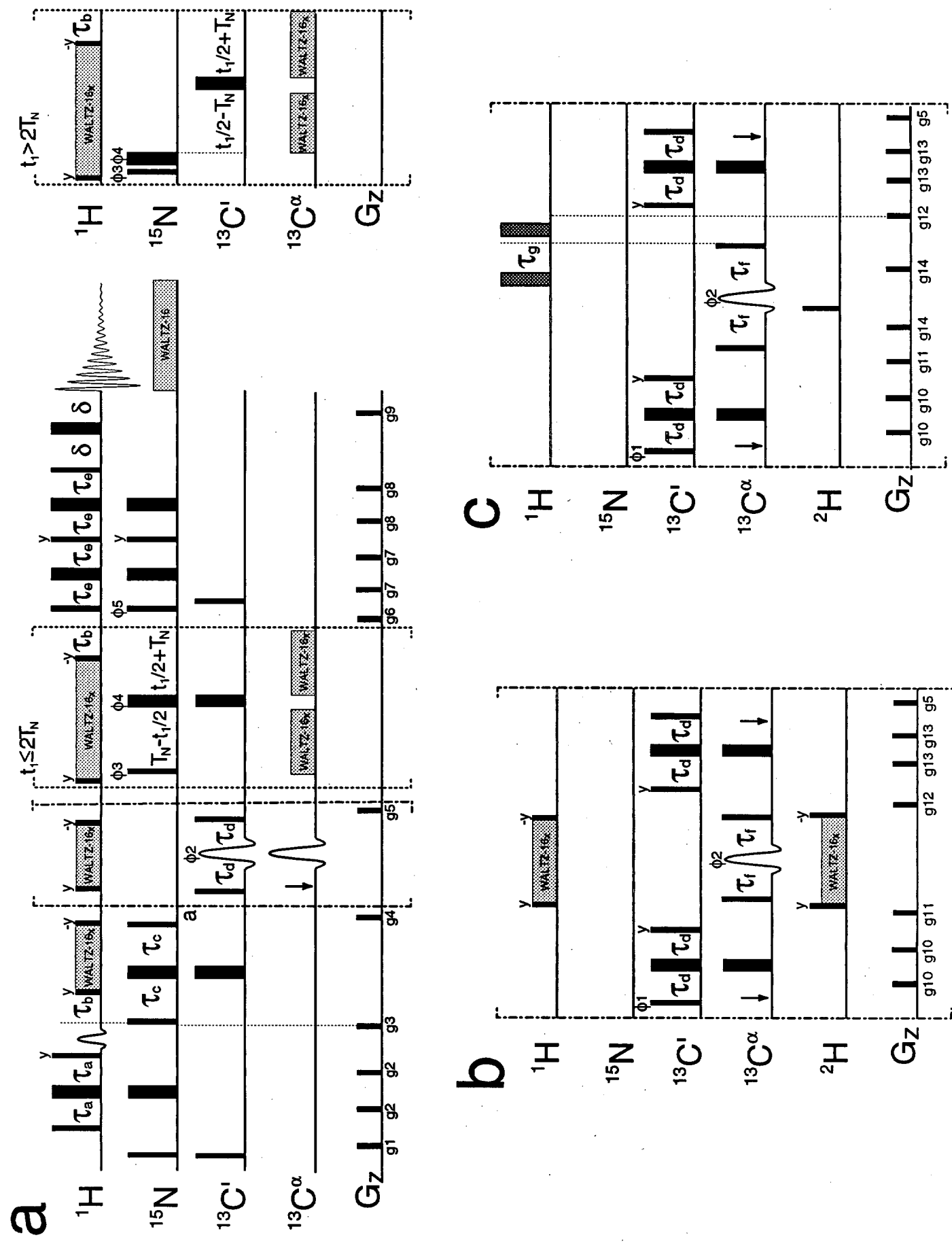


Supplemental Figure



Supplemental Figure. Pulse schemes used to measure (a) $^{13}\text{C}^\alpha\text{-}^{13}\text{C}'$, (b) $^{13}\text{C}^\alpha\text{-}^{13}\text{C}^\beta$ and (c)

$^{13}\text{C}^\alpha\text{-}^1\text{H}^\alpha$ dipolar couplings. $^{13}\text{C}^\alpha\text{-}^{13}\text{C}^\beta$ and $^{13}\text{C}^\alpha\text{-}^1\text{H}^\alpha$ couplings are obtained from sequences

in which the dash-dot portion in (a) is replaced by the schemes in (b) and (c),

respectively. All are HNCO-based sequences¹ which yield sets of $^{15}\text{N}\text{-}^1\text{H}$ correlation

spectra in which the intensity of each peak (residue i) is modulated by the backbone

coupling from residue i-1. Magnetization of interest is passed from a backbone amide

proton to the directly coupled nitrogen and subsequently to the carbonyl of the previous

residue by INEPT transfers² and, at point a in the sequence, it is of the form $2C_z'N_z$. In

the $^{13}\text{C}^\alpha\text{-}^{13}\text{C}'$ pulse scheme (a) carbonyl magnetization is subsequently allowed to evolve

with respect to $^{13}\text{C}'\text{-}^{13}\text{C}^\alpha$ couplings for a period of $2\tau_d$. Magnetization is then labeled with

the ^{15}N chemical shift in a semi-constant time fashion^{3,4} and returned to the amide proton

for detection with preservation of equivalent pathways for enhanced sensitivity⁵⁻⁷. In the

$^{13}\text{C}^\alpha\text{-}^{13}\text{C}^\beta$ variant of the sequence (b) the value of τ_d is fixed at approximately $\frac{1}{4(^1J_{C\alpha-C'})}$ so

that, after the period of $2\tau_d$, the relevant magnetization is of the form $4C_z'N_zC_z^{*\alpha}\text{-}^{13}\text{C}^\alpha$

magnetization is then allowed to evolve with respect to $(^1J_{C\alpha-C\beta} + ^1D_{C\alpha-C\beta})$ for a variable

delay of $2\tau_f$ and returned to the amide proton as above. A TROSY-based⁸ version of this

experiment has recently been applied to studies of the *E. coli* maltose binding protein⁹

and the interested reader may refer there for more detailed discussion. In the $^{13}\text{C}^\alpha\text{-}^1\text{H}^\alpha$

experiment (scheme c) τ_f is set to $\frac{1}{2(^1J_{C\alpha-C\beta})}$ and $^{13}\text{C}^\alpha$ magnetization is allowed to evolve

with respect to proton couplings for a period of $2\tau_g$. In the samples used for these experiments approximately 50% of residues are deuterated at the C^α position. Signal from $^{13}\text{C}^\alpha$ - $^2\text{H}^\alpha$ spin pairs is partially suppressed by a ^2H 90° pulse at the midpoint of the carbon constant time period which converts the outer two lines of the ^{13}C triplet into non-refocused multiple quantum coherences¹⁰. The ^1H , ^{15}N , ^{13}C and ^2H carriers are centered at 4.73, 119, 176 and 4.5 ppm, respectively. All ^1H pulses are applied with a field strength of 31 kHz, with the exception of the water selective flip back pulse prior to gradient g3 which is 1.7 ms in duration and the pulses flanking the WALTZ decoupling elements¹¹ (and the elements) where a field of 6.4 kHz is employed. The shaded 180° pulses are of the composite variety¹². ^{15}N pulses are applied using a 6 kHz field, with a 1 kHz WALTZ-16 decoupling field during acquisition. All ^{13}C 90° (180°) rectangular pulses are applied at a field strength of $\Delta/\sqrt{15}$ ($\Delta\sqrt{3}$), where Δ is the separation (Hz) between the centers of the $^{13}\text{C}^\alpha$ and $^{13}\text{C}^\beta$ chemical shift regions¹. The $^{13}\text{C}^\alpha$ shaped pulse in scheme (a) has the G3 profile¹³ (400 μs , centered at 58 ppm) and in schemes (b) and (c) the REBURP profile¹⁴ (400 μs , centered at 43 and 58 ppm, respectively) with a REBURP shape (400 μs) also employed for the $^{13}\text{C}^\beta$ shaped pulse in sequence (a). $^{13}\text{C}^\alpha$ decoupling is achieved using a 118 ppm modulated WALTZ-decoupling element where each of the 90°

pulses has the SEDUCE-1 profile¹⁵ (330 μ s). The vertical arrows indicate the positions of Bloch-Siegert compensation pulses¹⁶ (i.e., the $^{13}\text{C}^\alpha$ shaped pulse is applied after the $^{13}\text{C}^\alpha$ pulse in sequence (a), while the $^{13}\text{C}^\alpha$ pulse is applied after (before) the $^{13}\text{C}^\alpha$ pulse during the first (second) $2\tau_d$ period in schemes (b) and (c). ^2H decoupling is as described in the legend to Figure 1. The delays employed are: $\tau_a=2.3$ ms; $\tau_b=5.5$ ms; $\tau_c=14$ ms; $T_N=14$ ms; $\tau_e=2.3$ ms; $\delta=500$ μ s. The delay τ_d is varied when recording spectra using scheme (a) ($^{13}\text{C}^\alpha$ - $^{13}\text{C}^\alpha$ dipolar couplings) while $\tau_d=4.1$ ms in schemes (b) and (c). τ_f is varied in experiments recorded with sequence (b) ($^{13}\text{C}^\alpha$ - $^{13}\text{C}^\beta$ couplings) while $\tau_f=14$ ms in sequence (c). In this case ($^{13}\text{C}^\alpha$ - $^1\text{H}^\alpha$ couplings) the value of τ_g is varied between experiments (see Materials and Methods). The phase cycle employed is, scheme (a): $\phi 2=x, y, -x, -y$; $\phi 3=4(x), 4(-x)$; $\phi 4=x, -x$; $\phi 5=x$ rec=2(x, -x), 2(-x, x); schemes (b), (c): $\phi 1=x, -x$; $\phi 2=2(x), 2(y), 2(-x), 2(-y)$; $\phi 3=8(x), 8(-x)$; $\phi 4=x, -x$; $\phi 5=x$; rec=2(x, -x, -x, x), 2(-x, x, x, -x). Quadrature detection in t_1 (^{15}N) is achieved with the gradient enhanced sensitivity approach^{6,7} in which two separate data sets are recorded for each t_1 increment with 180° added to $\phi 5$ and the sign of gradient g9 inverted for the second set. The phase $\phi 3$ is incremented by 180° in concert with the receiver for each complex t_1 point¹⁷. The gradients used are: $g1=(0.5\text{ms}, 8\text{G/cm})$; $g2=(0.5\text{ms}, 4\text{G/cm})$; $g3=(1.0\text{ms}, 10\text{G/cm})$; $g4=(0.8\text{ms}, 15\text{G/cm})$; $g5=(0.6\text{ms}, 10\text{G/cm})$; $g6=(1.25\text{ms}, 30\text{G/cm})$; $g7=(0.3\text{ms}, 4\text{G/cm})$;

g8=(0.4ms, 2G/cm); g9=(0.125ms, 29.6G/cm); g10=(1.0ms, 7G/cm); g11=(1.0ms, 15G/cm); g12=(1.0ms, 8G/cm); g13=(1.0ms, 4G/cm); g14=(0.2ms, 30G/cm).

References

- 1) Kay, L. E.; Ikura, M.; Tschudin, R.; Bax, A. *J. Magn. Reson.* **1990**, *89*, 496-514.
- 2) Morris, G. A.; Freeman, R. *J. Am. Chem. Soc.* **1979**, *101*, 760-762.
- 3) Logan, T. M.; Olejniczak, E. T.; Xu, R. X.; Fesik, S. W. *J. Biomol. NMR* **1993**, *3*, 225-231.
- 4) Grzesiek, S.; Bax, A. *J. Biomol. NMR* **1993**, *3*, 185-204.
- 5) Palmer, A. G.; Cavanagh, J.; Wright, P. E.; Rance, M. *J. Magn. Reson.* **1991**, *93*, 151-170.
- 6) Kay, L. E.; Keifer, P.; Saarinen, T. *J. Am. Chem. Soc.* **1992**, *114*, 10663-10665.
- 7) Schleucher, J.; Sattler, M.; Griesinger, C. *Angew. Chem. Int. Ed. Engl.* **1993**, *32*, 1489-1491.
- 8) Pervushin, K.; Riek, R.; Wider, G.; Wüthrich, K. *Proc. Natl. Acad. Sci. USA* **1997**, *94*, 12366-12371.
- 9) Evenas, J.; Mittermaier, A.; Yang, D.; Kay, L. E. *J. Am. Chem. Soc.* **2001**, *123*, 2858-2864.
- 10) Gardner, K. H.; Rosen, M. K.; Kay, L. E. *Biochemistry* **1997**, *36*, 1389-1401.

- 11)Shaka, A. J.; Keeler, J.; Frenkiel, T.; Freeman, R. *J. Magn. Reson.* **1983**, *52*, 335-338.
- 12)Levitt, M.; Freeman, R. *J. Magn. Reson.* **1978**, *33*, 473-476.
- 13)Emsley, L.; Bodenhausen, G. *Chem. Phys. Lett.* **1987**, *165*, 469-476.
- 14)Geen, H.; Freeman, R. *J. Magn. Reson.* **1991**, *93*, 93-141.
- 15)McCoy, M. A.; Mueller, L. *J. Am. Chem. Soc.* **1992**, *114*, 2108-2112.
- 16)Vuister, G. W.; Bax, A. *J. Magn. Reson.* **1992**, *98*, 428-435.
- 17)Marion, D.; Ikura, M.; Tschudin, R.; Bax, A. *J. Magn. Reson.* **1989**, *85*, 393-399.